Full Length Research Paper

A comparative study of the defluoridation efficiency of synthetic dicalcium phosphate dihydrate (DCPD) and lacunar hydroxyapatite (L-HAp): An application of synthetic solution and Koundoumawa field water

A. S. Manzola[1,2]*, M. S. Laouali[1] and M. Ben Amor[2]

[1]Laboratoire de Chimie Analytique et Minérale, Faculté des Sciences et Techniques, Université Abdou Moumouni BP 10662, Niamey, Niger.
[2]Laboratoire des Traitements des Eaux Naturelles, CERTE, Technopôle de Borj Cedria, BP 273, 8020, Soliman, Tunisia.

This paper deals with the comparison of defluoridation efficiency of two defluoridation agents by the use of dicalcium phosphate dihydrate (DCPD) and lacunar hydroxyapatite (L-Hap) as a fluoride sorbents. The DCPD and L-HAp are characterized by using XRD and FTIR techniques. Defluoridation of synthetic solution of sodium fluoride (NaF) and natural waters of Koudoumawa are studied. The fluoride removal capacity is as follows: DCPD: (26.37 mg.g^{-1}; 0.0174 g, 9.81 mg.g^{-1}; 0.1012 g) and L-Hap: (18.96 mg.g^{-1}; 0.0174 g, 8.00 mg.g^{-1}; 0.1012 g). The optimum 0.0623 g of DCPD/100 mL dosage of synthetic solution could bring down the level of fluoride within the tolerance limit, [F⁻] = 0.38 mg/l (WHO guideline value = 0.8 mg/l), the pH rise is 5.10 and the defluoridation time is 72 h. For L-Hap, it is 0.1012 g of L-Hap/100 mL, [F⁻] = 1.98 mg/l in the same conditions. For Koundoumawa natural waters, 0.0527 g of L-Hap/100 mL of solution could bring down the level of fluoride, [F⁻] = 0.84 mg/l. New mechanisms of fluoride removal by DCPD and L-HAp are proposed from which it is established that this material removes fluoride by ion-exchange, adsorption process, dissolution, precipitation and co-precipitation.

Key words: Defluoridation, dicalcium phosphate dihydrate (DCPD), lacunar hydroxyapatite (L-Hap), adsorption, ion-exchange, dissolution-precipitation.

INTRODUCTION

To provide water requirements for the rural population and to fight against poverty, Niger government exploits waters from wells and drillings. In 1996, more than 6207 drillings and 10005 wells were done. These drillings play

Table 1. Physicochemical composition of Koundoumawa waters.

Parameter	pH	Conductivity (µS.cm⁻¹)	Concentrations (mg/l)								
			Ca^{2+}	Mg^{2+}	Na^+	K^+	SO_4^{2-}	HCO_3^-	NO_3^-	NO_2^-	F^-
Koundoumawa well water (summer)	7.1	384	42.1	24.45	87	5	25	216.08	8	0.02	4
Koundoumawa well water (rainy)	7	381	20.8	03	85	06	20	200.1	28	0.28	2.3
Koundoumawa drilled water	7.5	379	39.1	22.15	69	03	29	216.70	9	0.01	5

a primary role in water supply to the rural population. More than 90% of rural population in Niger depends on underground water as their drinking waters sources and fluoride excess is generally found in underground waters. A study carried out by the Ministry in charge of Waters, Environment and Fight against desertification (MHE/FAD) in 2005 on the physico-chemical analysis of raw water showed a high fluoride concentration according to World Health Organization (WHO) guidelines. WHO has set a guideline value of 0.8 mg/l for hot countries as the maximum permissible level of fluoride for drinking water to avoid health effects of fluoride water poisoning (WHO, 1996). In over a total of 211 studied drillings, 38% presented a fluoride concentration higher than 0.8 mg/l. The highest concentrations are recorded in Tibiri, Koundoumawa (in the Eastern part of Niger) and in Ingall (in the Northern part of Niger) with concentrations varying from 5 to 8 mg/l. Table 1 gives the chemical composition of Koundoumawa well and drilled waters during the summer rainy season. It has fluoride concentration of about 2 to 5 mg/l, its pH is about 7 to 7.5, and a bicarbonate concentration of about 167.7 to 216.08 mg/l.

A study carried out by UNICEF in 1998 classified Niger among the countries presenting fluorosis endemic contaminations. Several processes of defluoridation of drinking water have been reported in literature such as: ion-exchange, adsorption, and coagulation and precipitation process. Based on these processes, several defluoridation methods have been proposed by using nanosized hydroxyapatite (Yu et al., 2011), hydroxyapatite (Mourabet et al., 2011; Jiménez-Reyes and Solache-Ríos, 2010), surface coated hydroxyapatite powders (Subbaiah and Sankaran, 2014). Dicalcium phosphate dihydrate (DCPD) has been reported to be efficient for water defluoridation (Sekar et al., 2009; Masamoto and Tetsuji, 2004; Moubaret et al., 2011; Taewook et al., 2012). Several methods based on coconut shell carbon (Anirudhan et al., 2007; Amit et al., 2011), bone char (Medellin-Castillo et al., 2014), hybrid precipitation-microfiltration process (Nash and Liu, 2010), precipitated fluorhydroxyapatite nanoparticles (Kevin, 2014), Al (III) modified calcium hydroxyapatite, nano-hydroxyapatite/chitin composite (Yulun and Chun, 2012), alginate bioencapsulated nano-hydroxyapatite composite (Kalimuthu and Natrayasamy, 2014), and recently other defluoridation methods including membrane process based on reverse osmosis and nanofiltration (Simons, 1993; Rao et al., 1998; Mameri et al., 1998) and cellulose anhydroxyapatite nanocomposites (Xiaolin et al., 2013), glass derived hydroxyapatite (Wen et al., 2011), nano-hydroxyapatite/chitosan (Sundaram et al., 2008) were reported. Because of the socio-economic conditions in Niger, it is impossible to set up the defluoridation processes mentioned above. Thus, the rural populations are obliged to consume this fluoride poisoning water with its consequence, the appearance of the dental and skeletal fluorosis. The most dramatic example is the case of the children from Tibiri (Maradi, in the middle-east of Niger) where more than 450 children are affected by various forms of fluorosis, which include dental, skeletal and non-skeletal forms (Rapport Mission Internationale d'Enquête, 2002). However, for developing countries, precipitation and adsorption are the most accessible methods. Indeed the management and maintenance of current and proposed defluoridation technologies require expensive chemicals and/or a high level of technological skill and can be applied only in centralized water distribution systems (Rao et al., 1998). Precipitation methods are based on the addition of chemicals to water and removal of insoluble fluoride compounds as precipitates or co-precipitates or adsorbed onto the formed precipitates (Nash and Liu, 2010). In adsorption processes, fluoride is removed either by ion exchange, physical or surface chemical reactions with the adsorbent material. Hydroxyapatite (HAp) was used to remove cadmium, oxovanadium, cobalt, lead and zinc (Lusvardi et al., 2002; Vega et al., 2003; Hammari et al., 2004; Smiciklas et al., 2006; Sandrine et al., 2007). It appears

that with hydroxyapatite (HAp), the adsorption and ion-exchange mechanisms are the most favorable mechanisms for fluoride removal (Meenakshi et al., 2007). The removal of fluoride using HAp has been reported earlier (Fan et al., 2003; Hammari et al., 2004). Sairam et al. (2008) have used nano-hydroxyapatites for water defluoridation. Lacunar hydroxyapatite or calcium-deficient hydroxyapatite (CDHA) nano-crystals incorporated with bovine serum albumin (BSA) to form BSA-loaded nano-carriers were synthesized via both *in situ* and *ex situ* processes (Tse-Ying et al., 2005). Spherical Ca-deficient hydroxyapatite (HA) granules are expected to be useful drug carriers in bony sites because of their bone regeneration and adsorption ability (Masanobu et al., 2013). To study the effects of nanocrystalline calcium deficient hydroxyapatite incorporation in glass ionomer cements, bioactive nanocrystalline calcium deficient hydroxyapatite (nCDHA) with improved mechanical and resorption properties was synthesized (Sumit et al., 2011). The objective of the present study was to investigate the performance of synthesized DCPD and Lacunar hydroxyapatite as feasible and suitable adsorbent. Synthesized L-HAp and DCPD are synthesized in the laboratory by precipitation method. Defluoridation studies are carried out under various equilibrating conditions like the amount of adsorbent, the effect of contact time and the pH. Detailed precisions during the defluoridation mechanism by L-HAp and DCPD and the kinetic studies are presented.

EXPERIMENTAL SET UP AND PROCEDURES

Synthesis of DCPD and L-Hap

The synthesis of L-HAp and DCPD involved adding variable volumes of 0.1 M of monosodium phosphate dihydrate to 100 mL of 0.025 M of calcium chloride monohydrate in a closed tricol balloon reaction vessel. The calcium phosphate precipitation is being controlled by the pH level adjustment with 1 M NaOH solution, using a pH-meter TACUSSEL giving an accuracy of 0.01 unit of pH. The synthesis of DCPD involves the reaction of calcium chloride monohydrate and monosodium phosphate dihydrate with a Ca/P ratio close to 1. pH level of the reaction should be maintained at pH ranging from 5.8 to 6.6 (Manzola et al., 2013), otherwise it may lead to the formation of OH-Apatite (Legeros et al., 1983; Casciani et al., 1980). From pH 7 to 7.8 it precipitates Lacunar hydroxyapatite (L-Hap) (Manzola et al., 2013). The medium agitation is carried out using a magnetic stick at the ambient temperature of 22 to 25°C. The precipitated solution is poured into a 250 mL bottle and kept for 1, 3 or 7 days, then filtered. The precipitated solid is dried from 60 and 70°C for 24 h to get DCPD ($CaHPO_4.2H_2O$) or L-Hap.

Characterisation of DCPD and L-Hap

The solid phases obtained at different pH are characterized by powder X-ray diffraction (XRD) and the phase identification is made

by using a JCPDS cards (Joint Committee on Powder Diffraction Standards) and Fourier Transform Infrared Spectrometer (FTIR). The XRD patterns are obtained by using a PW 1050/37 diffractometer with a monochromatic radiation Kα1 of Cu (λ = 1.5418; 1.5405 A°). The FTIR spectra are performed by using the KBr pellet technique in a Shimadzu Fourier Transform-8300 in the range of 4500-400 cm^{-1} at a resolution of 4 cm^{-1}. Also, the results of FTIR spectrometer and XRD are used to confirm the fluoride uptake by the DCPD or L-Hap precipitates.

Adsorption experiments

Synthetic solution

The fluoride experimental solutions are prepared by a quantitative dilution of stock solution. The stock solution of 1000 mg/l fluoride is obtained by dissolving an appropriate amount of sodium fluoride in distilled water.

A 100 ml of the fluoride experimental solution (10 mg/l as initial fluoride concentration) is taken into a 150 mL of PVC conical flask and a known weight of adsorbent material (0.0174; 0.0318; 0.0527; 0.0623 and 0.1012 g) is added in this solution, and then kept for stirring at 150 rpm on a horizontal rotary shaker for 0; 2; 21; 48; 72 and 92 h in order to reach the equilibrium. After that, the solution is then filtered through Millipore filter paper 22 μm and the filtrate is analyzed for residual fluoride concentration by ion selective electrode (ISE) using field ion meter 340I/ION. In order to regulate the total ionic strength, the TISAB adjusting buffer is added to the sample and standard solutions. The TISAB buffer was added in order to maintain pH constant, to decomplex metal-F complexes contained in the sample during measurement and allowed us to get the total free fluoride concentration in the solution. The fluoride removal experiments are studied over different operational conditions including effect of adsorbent dose, the nature of adsorbent and the effect of contact time. All the experiments were carried out at 30°C, room temperature. During the experiments, the fluoride ion concentration and the pH solution were recorded.

Fluoride poisoning field water of Koundoumawa

In the second serial experiments, the fluoride removal ability of L-HAp and DCPD was tested in field water collected from KOUNDOUMAWA drilling (Zinder, in the far eastern part of Niger) at the same conditions as the synthetic water. The physicochemical characteristics of field water samples are determined before batch adsorption study. The detailed characteristics of field waters are given in Table 1.

RESULTS AND DISCUSSION

Characterization of DCPD sorbent

In order to characterize DCPD, XRD and FTIR were carried out on precipitated DCPD and DCPD samples mixed with fluoride solution. The XRD patterns of precipitated DCPD and the DCPD samples mixed with fluoride solution are respectively presented in Figures 1 and 2.
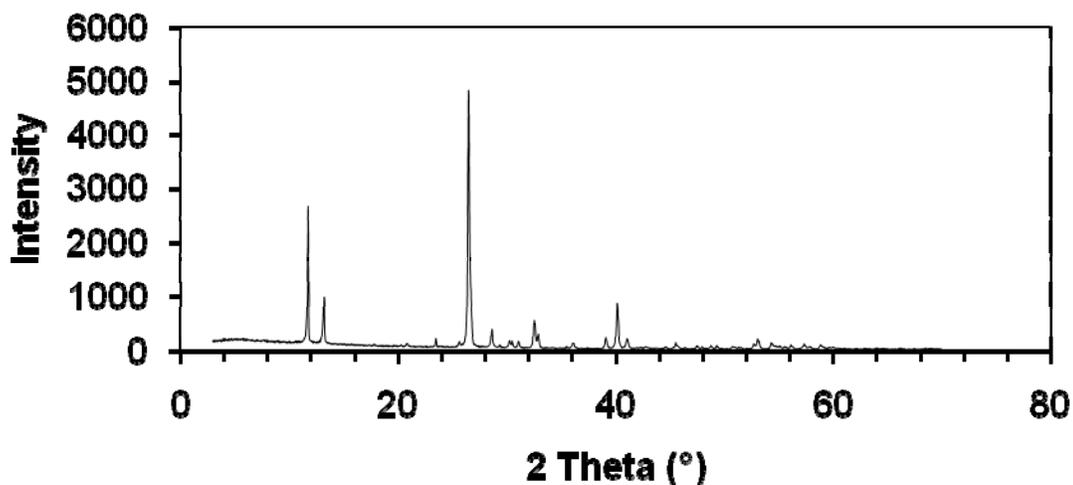
**Figure 1.** XRD patterns of precipitated DCPD.
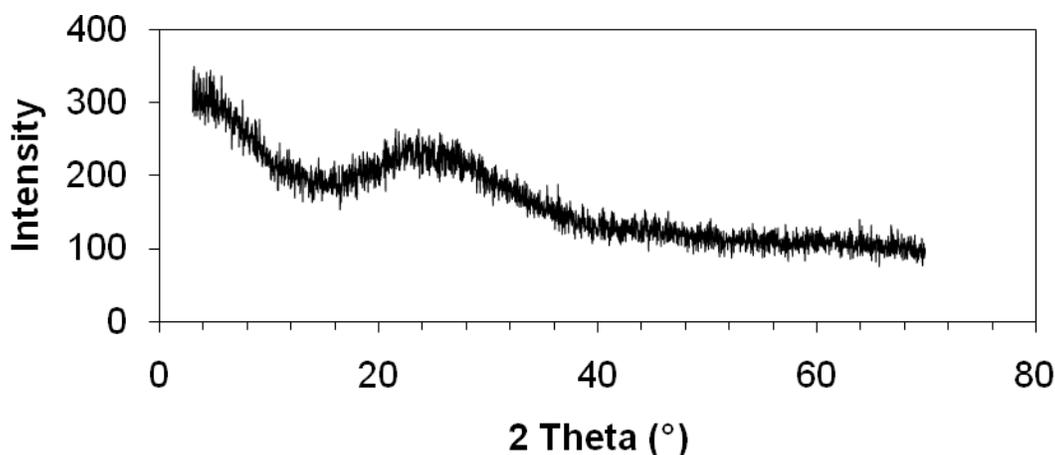
Figure 2. XRD patterns of fluoride sorbed precipitated DCPD.

The identification of crystal phases was done by using a JCPDS cards (Joint Committee on Powder Diffraction Standards). The XRD patterns shown in Figure 1 indicates the DCPD peaks at 2θ values of about 11.6°, 13.2°, 20.9°, 23.6°, 26.5°, 29.3° which are in the JCPDS cards (card number 09–0077). The maximum peak intensity is 26.5 degree theta. The spectra confirmed that the products obtained are mainly composed of the DCPD form of calcium phosphate (Figure 1). There is a meaningful change in the XRD patterns of DCPD after treatment with fluoride (Figure 2). The results of X-ray diffraction of treated product show amorphous product. Similar results are reported (Larsen et al., 1993) while studying the fluoride sorption on brushite, calcium

hydroxide, and bone char. The fine powder obtained was poorly crystallized apatite.

Figure 3 represents FTIR spectra of the samples before and after treatment with fluoride. In Figure 3, the absorption peaks appeared at 3540 and 3488 cm^{-1}, characteristics of valence vibrations of free H_2O (ν_{H_2O}), at 3290 and 3161 cm^{-1}, characteristics of valence vibrations of associated H_2O (ν_{H_2O}), at 2367 cm^{-1}, characteristic of valence vibrations ν_{O-H} of HPO_4^{2-} groups, at 1649 cm^{-1} characteristic of valence vibrations of H_2O of constitution (ν_{H_2O}), at 1220 and 790 cm^{-1}, characteristics of bond elongation vibrations δ_{P-O-H} at 1135, 1059 and 985 cm^{-1}, characteristics of valence vibrations ν_{PO} at 873 cm^{-1},
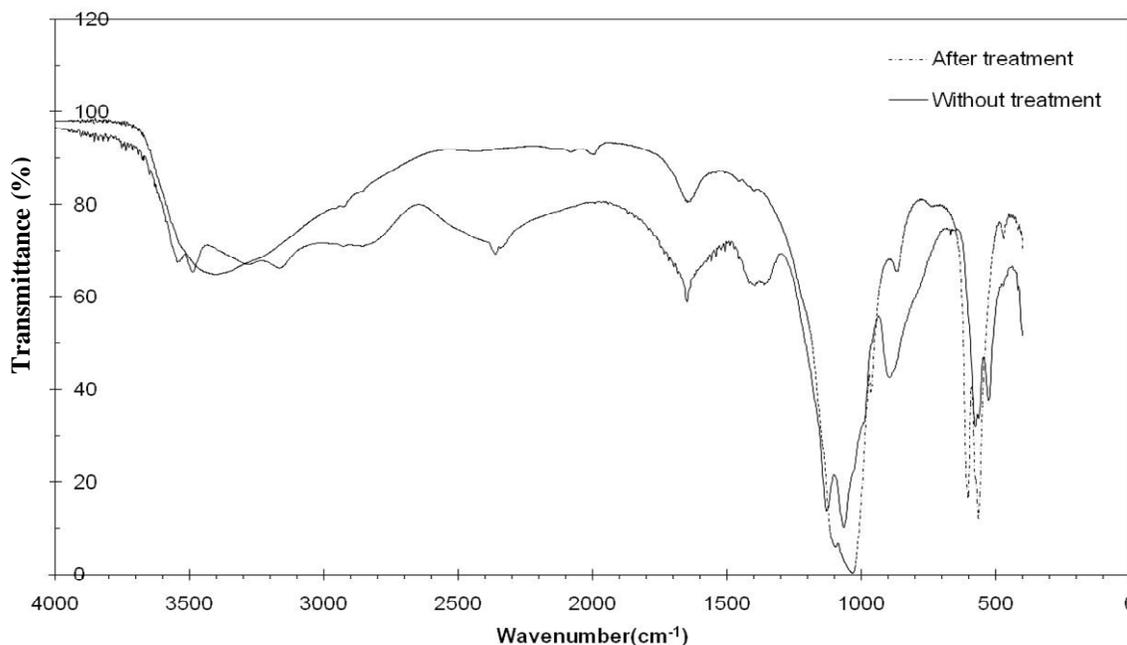
Figure 3. FTIR spectra of DCPD (without treatment and after treatment with fluoride).

characteristics of valence vibrations ν_{P-OH} and at 525 cm^{-1}, characteristics of valence vibrations ν_{O-P-O} (Legeros et al., 1983; Casciani et al., 1980). We can observe that the spectrum of precipitated solid is perfectly identical to infra-red spectrum of $CaHPO_4 \cdot 2H_2O$ (Legeros et al., 1983), and the characteristic bands are in conformity with those obtained (Legeros et al., 1983; Casciani et al., 1980).

There is a meaningful change in the FTIR spectrum of the sample after treatment with fluoride. In the presence of F$^-$ ions, the DCPD is transformed into ″OH-Apatite″, then into fluorinated hydroxyapatite FAp (Maiti et al., 1981; Takahashi et al., 1978). Indeed for the infra-red spectrum of ″OH-Apatite″ (Legeros et al., 1983; Casciani et al., 1980), absorption peaks appeared at 3561 cm^{-1} characteristics of valence vibrations of ν_{OH^-}, at 3473 cm^{-1} characteristic of valence vibrations ν_{H-O-H} of free H_2O, at 1647 cm^{-1} characteristic of valence vibrations ν_{H-O-H}, at 1112, 1033 and 960 cm^{-1} characteristic of valence vibrations $\nu_{PO_4^{3-}}$, at 873 cm^{-1} characteristic of valence vibrations ν_{P-OH}, at 602 and 562 cm^{-1} characteristics of elongation vibrations $\delta_{PO_4^{3-}}$. The apparition of two new bands at 775 and 468 cm^{-1} may be due to the fluoride adsorption/exchange, indicating the incorporation of fluoride into the solid.

Characterization of L-Hap sorbent

The identification of crystal phases was done by using a JCPDS cards (Joint Committee on Powder Diffraction Standards). The crystalline peaks at 2θ = 25.9°, 32°, 33° and 40° (Figure 4) indicating the L-Hap peaks which are in the JCPDS cards (card number 9-432). The maximum peak intensity is 32 degree theta. The spectra confirmed that the products obtained are mainly composed of the L-Hap form of calcium phosphate (Figure 4). There is no significant change in the XRD pattern of L-HAp after treatment with fluoride (Figure 5). Similar results were reported (Diaz-Nava et al., 2002) while studying the fluoride sorption on zeolites.

In Figure 6, there is a meaningful change in the FTIR spectrum of the sample after treatment with fluoride. The presence of F$^-$ ions makes the L-Hap transformed into fluorinated hydroxyapatite FAp (Maiti et al., 1981; Takahashi et al., 1978). For the infra-red spectrum of ″OH-Apatite″ (Legeros et al., 1983; Casciani et al., 1980), absorption peaks appear at 3561 cm^{-1} characteristics of valence vibrations of ν_{OH^-}, at 3473 cm^{-1} characteristic of valence vibrations ν_{H-O-H} of free H_2O, at 1647 cm^{-1} characteristic of valence vibrations ν_{H-O-H}, at 1112, 1033 and 960 cm^{-1} characteristic of valence vibrations $\nu_{PO_4^{3-}}$, at 873 cm^{-1} characteristic of valence vibrations ν_{P-OH}, at 602
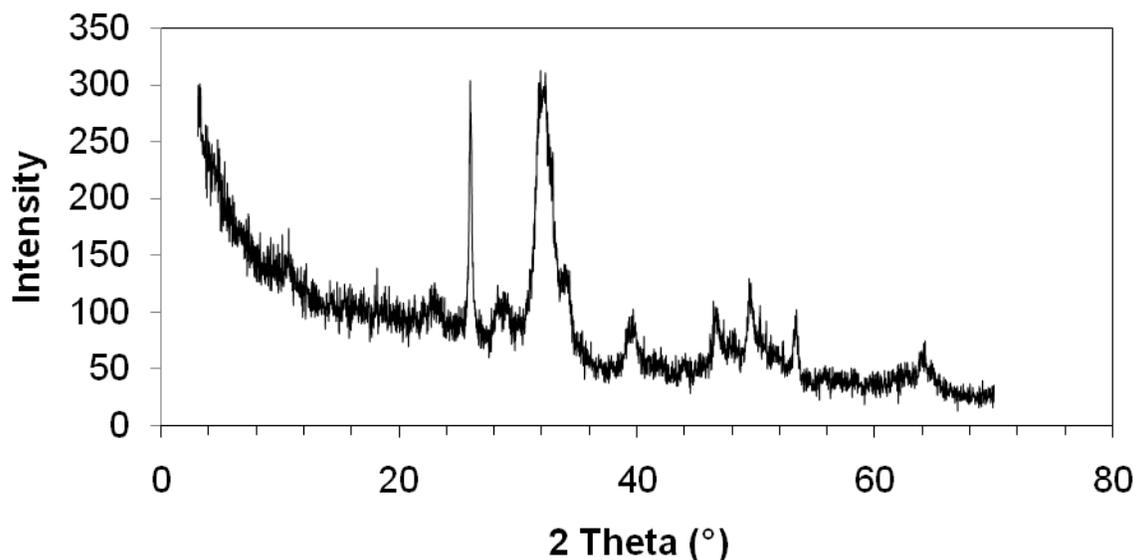
**Figure 4.** XRD patterns of precipitated L-HAp.
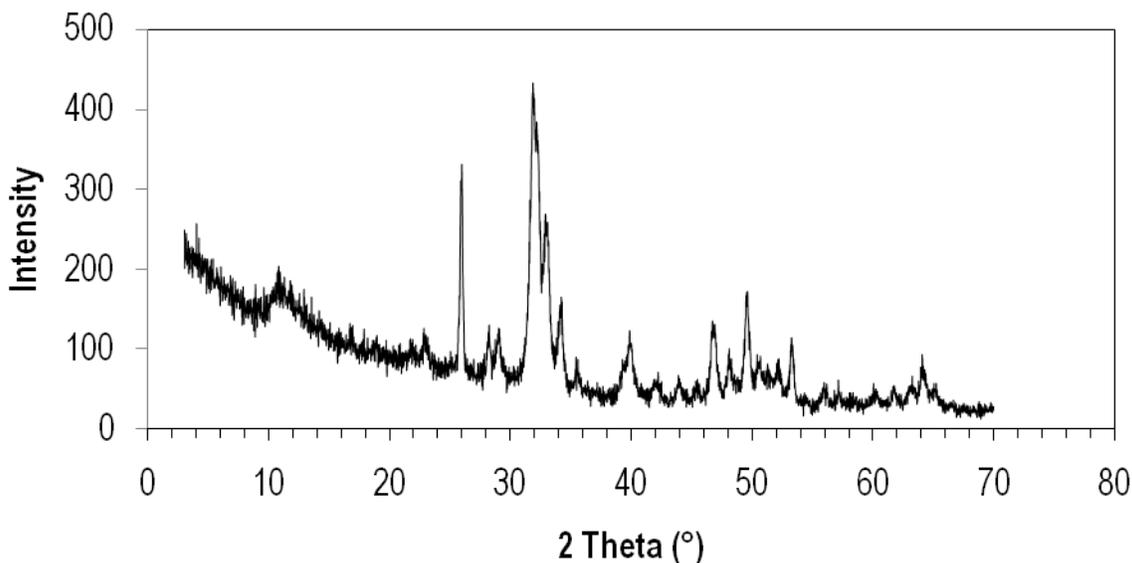
Figure 5. XRD patterns of fluoride sorbed precipitated L-HAp.

and 562 cm^{-1} characteristics of elongation vibrations $\delta_{PO4}{}^{3-}$. The presence of some OH$^-$ with F$^-$ disturbs the OH band frequencies of the pure calcium ″OH-Apatite″. There is a reduction in the intensity of OH bands at 3570 and 602 cm^{-1} with some displacement with lower frequencies in fluoride treated L-HAp which may be due to fluoride adsorption/exchange. The apparition of two new bands at 701 and 468 cm^{-1} for fluorinated

hydroxyapatite FAp may be due to the fluoride adsorption/exchange, indicating the incorporation of fluoride into the solid. It is known that FAp is more stable in solution than ″OH-Apatite″ (Chow et al., 1997). For the initial fluoride treated ″OH-Apatite″, the new band appears at 701 cm^{-1}. The displacement of the new band from 775 to 701 cm^{-1} confirms the formation of O–H⋯F bond in agreement with other authors (Okazaki et al.,
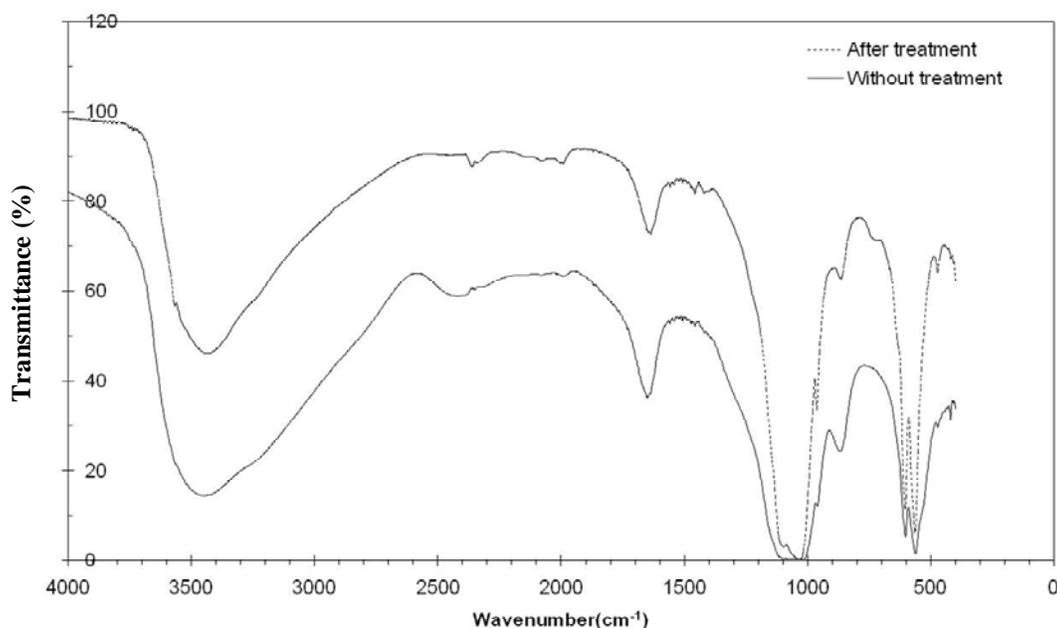
Figure 6. FTIR spectra of L-Hap (without treatment and after treatment with fluoride).

1981; Okazaki, 1992).

Adsorption experiments

Synthetic solution

DCPD sorbent - Effect of contact time and dose: In order to obtain the optimum DCPD sorbent dose defluoridation and contact time, experiments were carried out with various dosages of DCPD ranging from 0.0174 to 0.1012 g with 10 mg/l as initial fluoride concentration. We investigated the sorption of fluoride ion on DCPD as a function of contact time in the range of 0 to 92 h at room temperature and as a function of sorbent dose. The effect of fluoride removal capacity of DCPD with contact time and sorbent dose is shown in Figure 7. It was observed that fluoride removal capacity increases with contact time and contrary to the fluoride ion concentration (Figure 8), the fluoride removal capacity decreases with the raise of sorbent dose, where saturation is reached after 72 h for 0.0174; 0.0318; 0.0527 and 0.0623 g amount of DCPD sorbent dose. The maximum fluoride removal capacity is found to be 26.37 mg.g^{-1} at a sorbent dose of 0.0174 g. For 0.1012 g amount of DCPD sorbent dose, the fluoride removal capacity kept increasing and reached over 92 h 9.81 mg.g^{-1}. Indeed at low sorbent dose, the fluoride uptake capacity is high because of the better utilization of the available active sites and at high

sorbent dose, too many sites are available for limited quantity of fluoride and the lower equilibrium concentration of fluoride for sorption becomes negligible (Sanjay et al., 2009). Similar behavior has also been reported previously for other adsorbent (Kamble et al., 2007). The evaluation of fluoride ion concentration with contact time and sorbent dose is shown in Figure 8. We observed that the fluoride ion concentration decreased rapidly and continuously with the increase in the dose of the sorbent. This phenomenon was still observed for 72 h. From 72 to 92 h, it stayed steady for 0.0174; 0.0318; 0.0527 and 0.0623 g amount of DCPD sorbent dose. For 0.1012 g amount of DCPD sorbent dose, the fluoride ion concentration continued to decrease. For this amount, the concentration of fluoride ion reached for 92 h was [F$^-$] = 0.15 mg/l. The optimum dosage can be fixed as 0.0623 g for further studies as this dosage was found to bring down the level of fluoride within the tolerance limit, [F$^-$] = 0.38 mg/l for this amount (WHO guideline value = 0.8 mg/l). The steady state of DCPD sorbent was reached after 72 h for 0.0174; 0.0318; 0.0527 and 0.0623 g amount of DCPD sorbent dose. The uptake of fluoride can be controlled by adsorption or the dissolution-and-recrystallization mechanism. DCPD reached steady state only after 72 h, suggesting that the process is also governed by adsorption and mainly by dissolution-and-recrystallization mechanisms which are slow processes (Sairam et al., 2008; Meenakshi et al., 2007; Low et al., 1995; Taewook et al., 2012). For 0.1012 g amount of
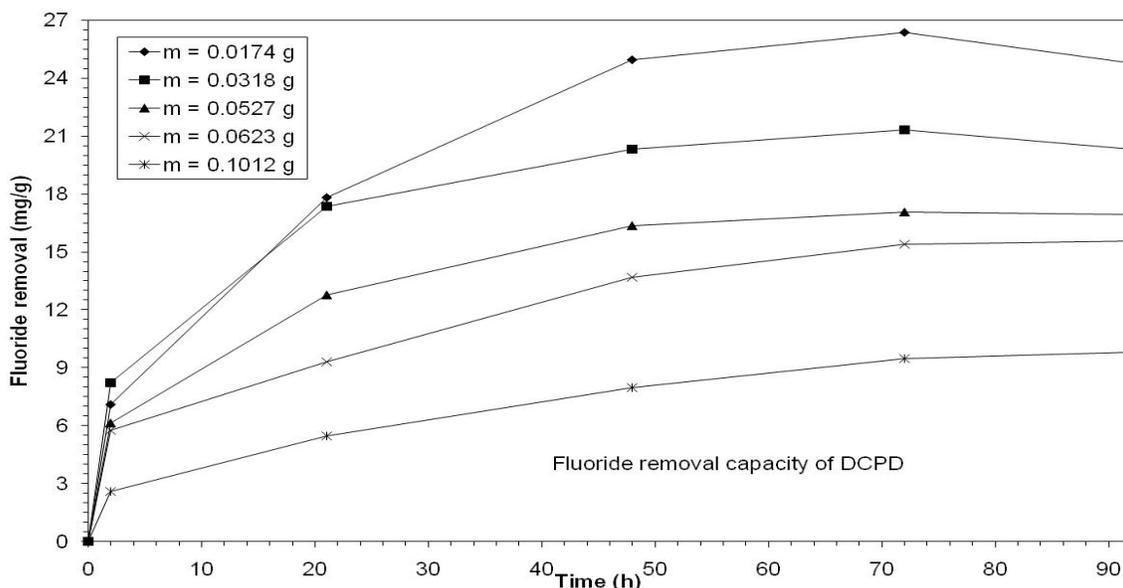
Figure 7. Effect of contact time and sorbent dose on the fluoride removal capacity of precipitated DCPD.
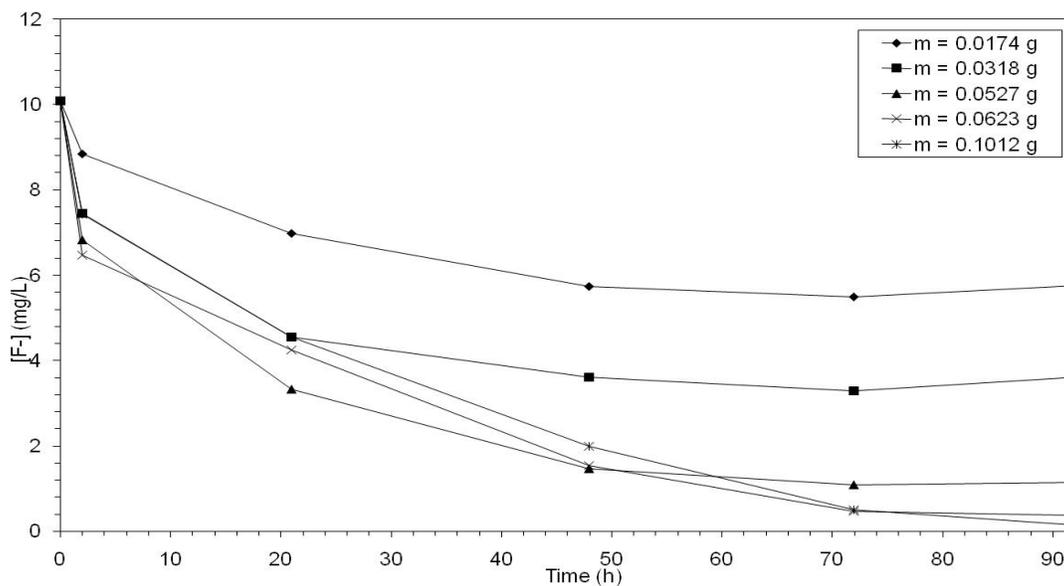

Figure 8. The evaluation of fluoride concentration during defluoridation: Effect of contact time and sorbent dose on precipitated DCPD.

DCPD sorbent dose, the steady state is not reached after 72 h.

Figure 9 shows the evaluation of the pH of the aqueous solution. The evaluation of pH fits the evaluation of fluoride ion concentration (Figure 9). We observed that the pH solution decreases rapidly and continuously with an increase in the dose of the sorbent (Lerch et al., 1966)

while studying the hydrolytic conversion of DCPD to apatite. Indeed in aqueous solution, the following reactions are proposed:

*Quick and partial dispersion of phosphate in aqueous medium:

$$CaHPO_4.2H_2O \Longleftrightarrow Ca^{2+} + HPO_4^{2-} + 2H_2O$$
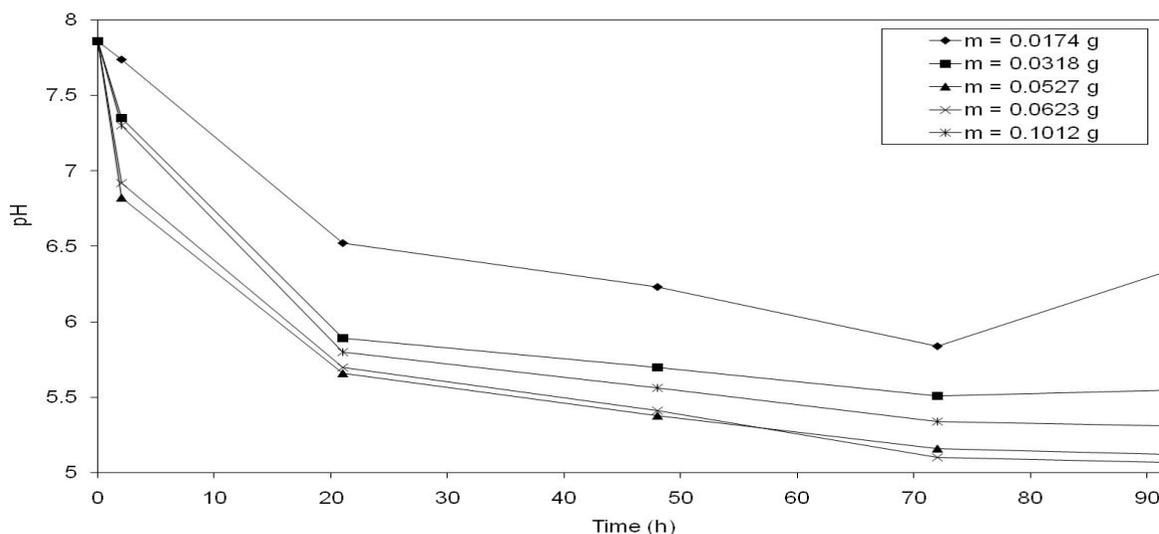
Figure 9. The evaluation of pH solution during the defluoridation: Effect of contact time and sorbent dose on precipitated DCPD.

*Quick hydrolytic conversion of HPO_4^{2-} ions:

$$HPO_4^{2-} + H_2O \Longleftrightarrow H_2PO_4^- + OH^-$$

*Low and concurential dismutation reaction:

$$2HPO_4^{2-} \Longleftrightarrow PO_4^{3-} + H_2PO_4^-$$

$$2HPO_4^{2-} + 2H_2O \Longleftrightarrow 2H_2PO_4^- + 2OH^-$$
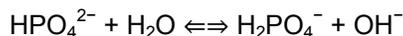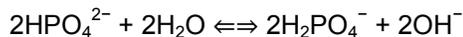
*Precipitation of PO_4^{3-} ions:

$$PO_4^{3-} + Ca^{2+} + HPO_4^{2-} + OH^- \Longleftrightarrow Apatitic\ calcium\ phosphate.$$
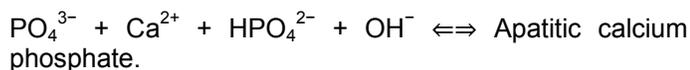
The decrease of pH is due to the presence of $H_2PO_4^-$ ions. Indeed this phosphate is acidic; its aqueous dissolution gives H_3PO_4 and a residual $CaHPO_4.2H_2O$ (Brown et al., 1959), reaches steady state at pH 5.5. In our experiments, DCPD reaches steady state after 72 h at pH 5.51 for 0.0318 g of sorbent; at pH 5.34 for 0.1012 g of sorbent; pH 5.16 for 0.0527 g of sorbent; pH 5.10 for 0.0623 g of sorbent. The pH solution plays an important role by controlling the adsorption at the water adsorbent interface and the dissolution-reprecipitation mechanism (Meenakshi et al., 1991). In the presence of fluoride ions and at these low pH, hydroxyapatite is faster when converted to fluorapatite because the solubility of the two salts differs increasingly with lower pH (Larsen et al., 1992). At high pH, the solubility of the two salts does not differ greatly (Featherstone et al., 1990), which explains why the uptake of fluoride in apatite is slow in this pH range. The dissolution of hydroxyapatite-reprecipitation of fluorapatite principle would be expected to operate most efficiently at low pH. As we have seen above, one disadvantage of such a defluoridation mechanism is that phosphate may be left in solution (the formation of H_3PO_4) and thus may favor bacterial growth.

L-Hap sorbent - effect of contact time and dose: In order to obtain the optimum L-Hap sorbent dose defluoridation and contact time, experiments were carried out with various dosages of L-Hap ranging from 0.0174 to 0.1012 g with 10 mg/l as initial fluoride concentration. We have investigated the sorption of fluoride ion on L-Hap as a function of contact time in the range of 0 to 72 h at room temperature and as a function of sorbent dose. The effect of fluoride removal capacity of L-Hap with contact time and sorbent dose is shown in Figure 10. It was observed that fluoride removal capacity increases with contact time and contrary to the fluoride ion concentration (Figure 11), the fluoride removal capacity decreases with increase in sorbent dose, where saturation is reached after 48 h for 0.0174; 0.0318; 0.0527 and 0.0623 g amount of L-Hap sorbent dose. The maximum of fluoride removal capacity is found to be 18.96 $mg.g^{-1}$ at a sorbent dose of 0.0174 g. For 0.1012 g amount of DCPD sorbent dose, the fluoride removal capacity stays increasing and reached 72 h for 8.00 $mg.g^{-1}$. Indeed at low sorbent dose, the fluoride uptake capacity is high because of the better utilization of the available active sites and at high sorbent dose, too many sites are available for limited quantity of fluoride and the lower equilibrium concentration of fluoride for sorption becomes negligible (Sanjay et al.,
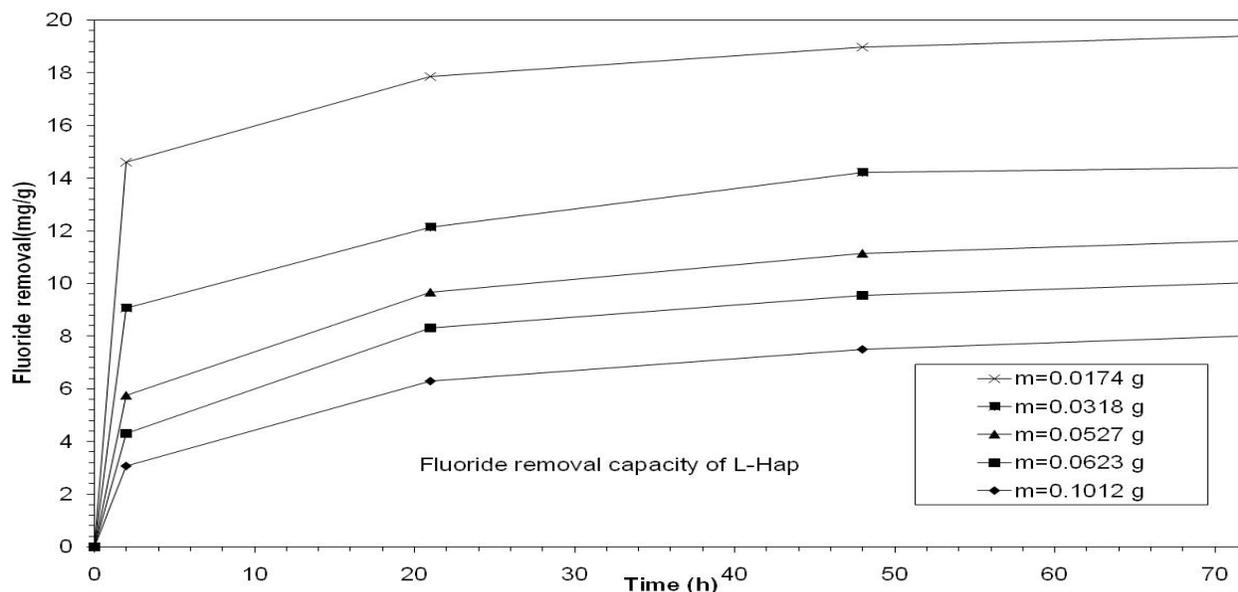
Figure 10. Effect of contact time and sorbent dose on the fluoride removal capacity of precipitated L-Hap.
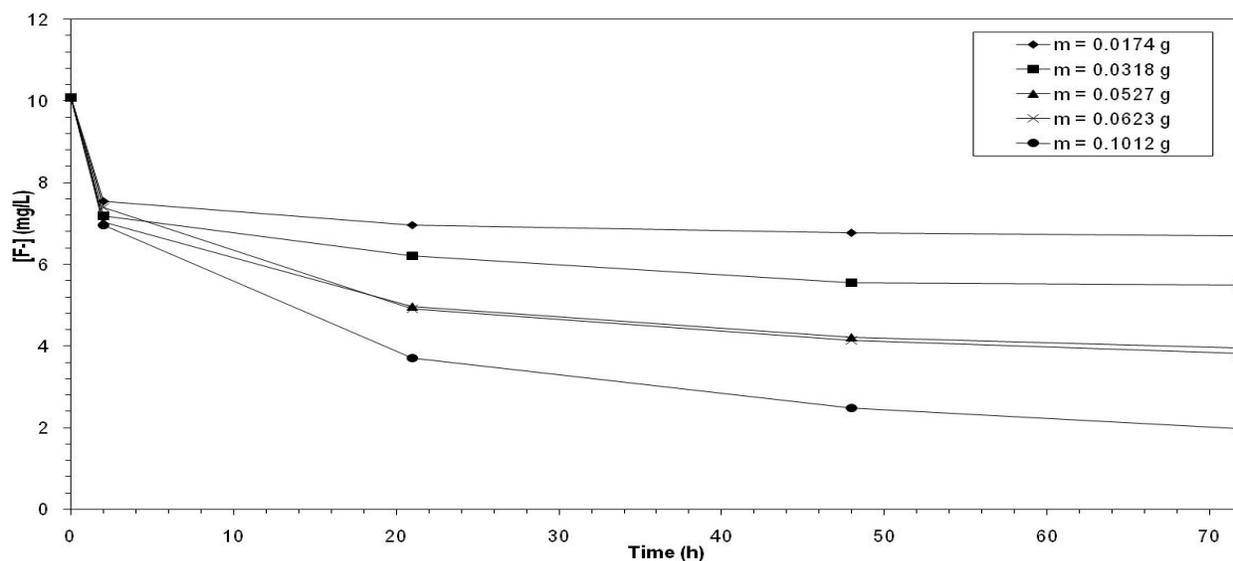

Figure 11. The evaluation of fluoride concentration during defluoridation: Effect of contact time and sorbent dose on precipitated L-HAp.

2009). Similar behavior has also been reported previously for other adsorbent (Kamble et al., 2007). The evaluation of fluoride ion concentration with contact time and sorbent dose is shown in Figure 11. We observed that the fluoride ion concentration decreases instantaneously and continuously within 2 hours, due to more active sites when increasing the dose of sorbent (Boualia et al.,

1993). Within the first two hours, the sorption process is essentially controlled by ion exchange mechanism because of the rapidity of the phenomenon and because of the pH solution increases instantaneously (Figure 12). This phenomenon can be described by the following reaction:

$$Ca_{10}(PO_4)_6(OH)_2 + 2F^- \Rightarrow Ca_{10}(PO_4)_6F_2 + 2OH^-$$
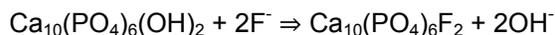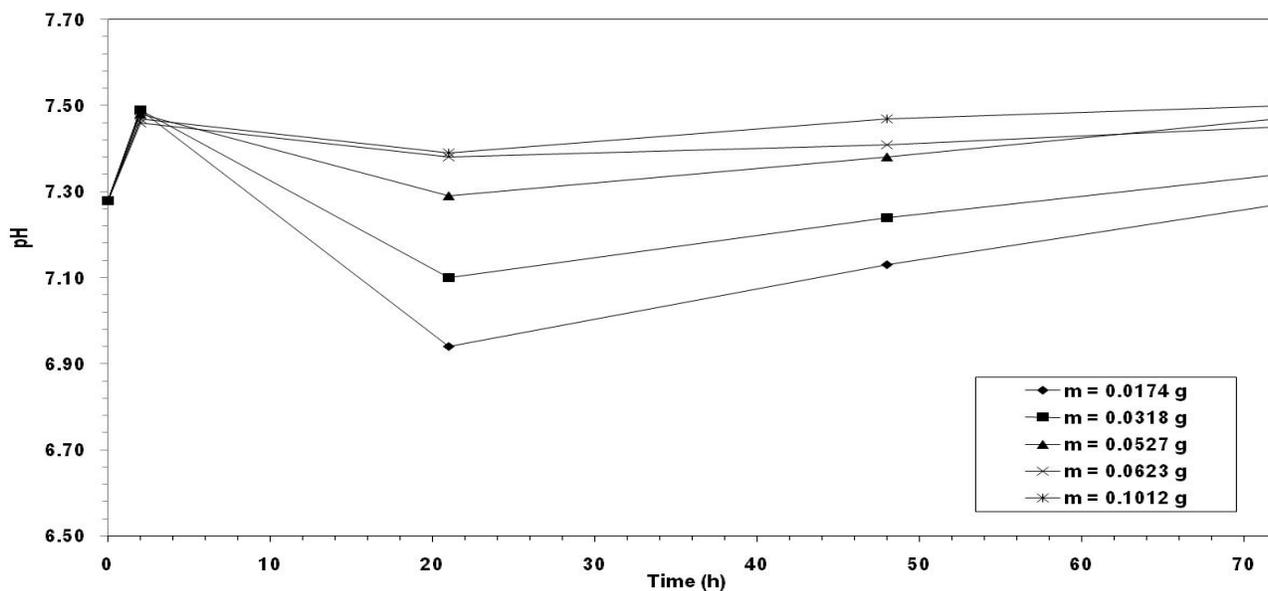
Figure 12. The evaluation of pH solution during the defluoridation: Effect of contact time and sorbent dose on precipitated L-HAp.

The uptake of fluoride can be controlled by adsorption or the dissolution-and-recrystallization mechanism. From 2 to 20 h, the fluoride ion concentration decreases with a slow rate with an increase in the dose of the sorbent, suggesting that the process is controlled by the dissolution-and-recrystallization mechanism because of the pH solution decreases in the same shape (Figure 12). This phenomenon can be described by the following reactions:

*Dissolution of Apatitic calcium phosphate:

Apatitic calcium phosphate $\Longleftrightarrow PO_4^{3-} + Ca^{2+} + HPO_4^{2-} + OH^-$

*Conversion of HPO_4^{2-} ions:

$2HPO_4^{2-} \Longleftrightarrow PO_4^{3-} + H_2PO_4^-$
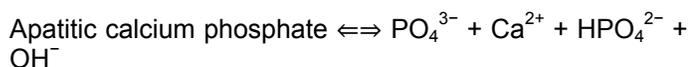
*Formation of fluoroapatite:

$10Ca^{2+} + 6PO_4^{3-} + 2F^- + H_2PO_4^- \Rightarrow Ca_{10}(PO_4)_6F_2 + H_2PO_4^-$
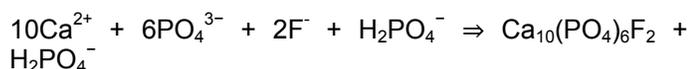
The decrease of pH is due to the presence of $H_2PO_4^-$ which renders the solution acidic (Brown et al., 1959). From 20 to 72 h, the fluoride ion concentration decreases with a average rate with the growth in the dose of the sorbent, suggesting that the process is again controlled by ion exchange mechanism because of the pH solution

increase in the same shape (Figure 11). This phenomenon can be described by the following reaction:

$Ca_{10}(PO_4)_6(OH)_2 + F^- \Rightarrow Ca_{10}(PO_4)_6FOH + OH^-$
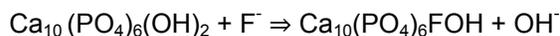
These schemes have been proposed by Sairam et al. (2008) without precision during the process. The fluoride ion concentration reached at 72 h is [F⁻] = 6.70 mg/l for 0.0174 g amount of L-Hap sorbent dose, [F⁻] = 5.5 mg/l for 0.0318 g amount of L-Hap sorbent dose, [F⁻] = 3.83 mg/l for 0.0623 g amount of L-Hap sorbent dose, [F⁻] = 3.83 mg/l for 0.0527 g amount of L-Hap sorbent dose and [F⁻] = 1.98 mg/l for 0.1012 g amount of L-Hap sorbent dose. According to these results, the minimum fluoride ion concentration reached at 72 his [F⁻] = 1.98 mg/l for 0.1012 g amount of L-Hap sorbent dose. This value does not satisfy the level of fluoride within the tolerance limit (WHO guideline value = 0.8 mg/l).

At high pH, the solubility of the two salts does not differ greatly (Featherstone et al., 1990) (Figure 12), which explains why the uptake of fluoride in apatite is slow in this pH range.

Fluoride poisoning Koundoumawa field water

A second set of tests, with fluoride poisoning Koundoumawa field water during rainy season (Table 1) ([F⁻] = 2.3 mg/l) has been performed in the laboratory at the same conditions as the synthetic water. With the aim
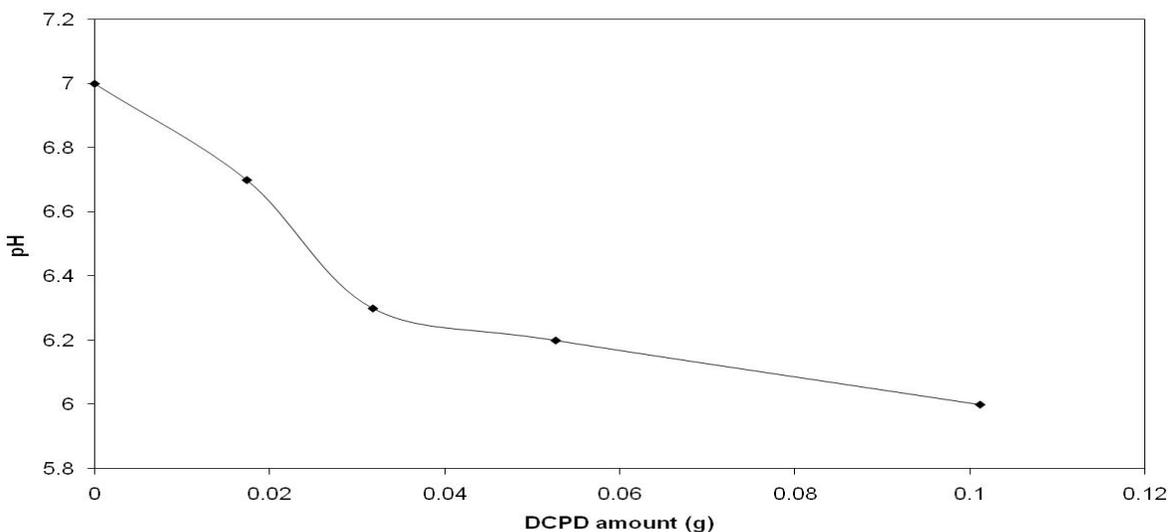
Figure 13. The evaluation of pH Koundoumawa field water during defluoridation: Effect of sorbent dose on precipitated DCPD.
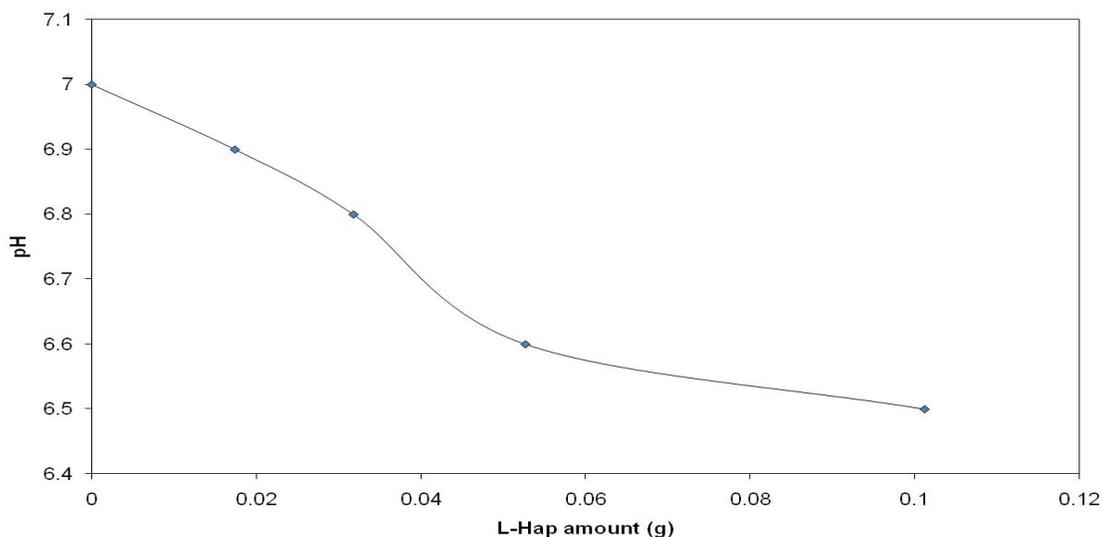

Figure 14. The evaluation of pH Koundoumawa field water during defluoridation: Effect of sorbent dose on precipitated L-HAp.

to obtain the maximum defluoridation, the contact time was fixed at 72 h. The results are presented in Figures 13, 14 and 15.

DCPD sorbent - Effect of amount: Figure 13 gives the evaluation of the pH of the aqueous solution. We observed that the pH solution decreases rapidly and continuously with increase in the dose of the DCPD sorbent. This phenomenon observed during synthetic solution defluoridation is in conformity with the observation (Lerch et al., 1966), suggesting that the process is controlled by the dissolution-and-recrystallization mechanism. The minimum pH obtained is 6.0 for 0.1012 g of sorbent.

L-Hap sorbent - Effect of amount: Figure 14 shows the evaluation of the pH of the aqueous solution. We observed that the pH solution decreases rapidly and
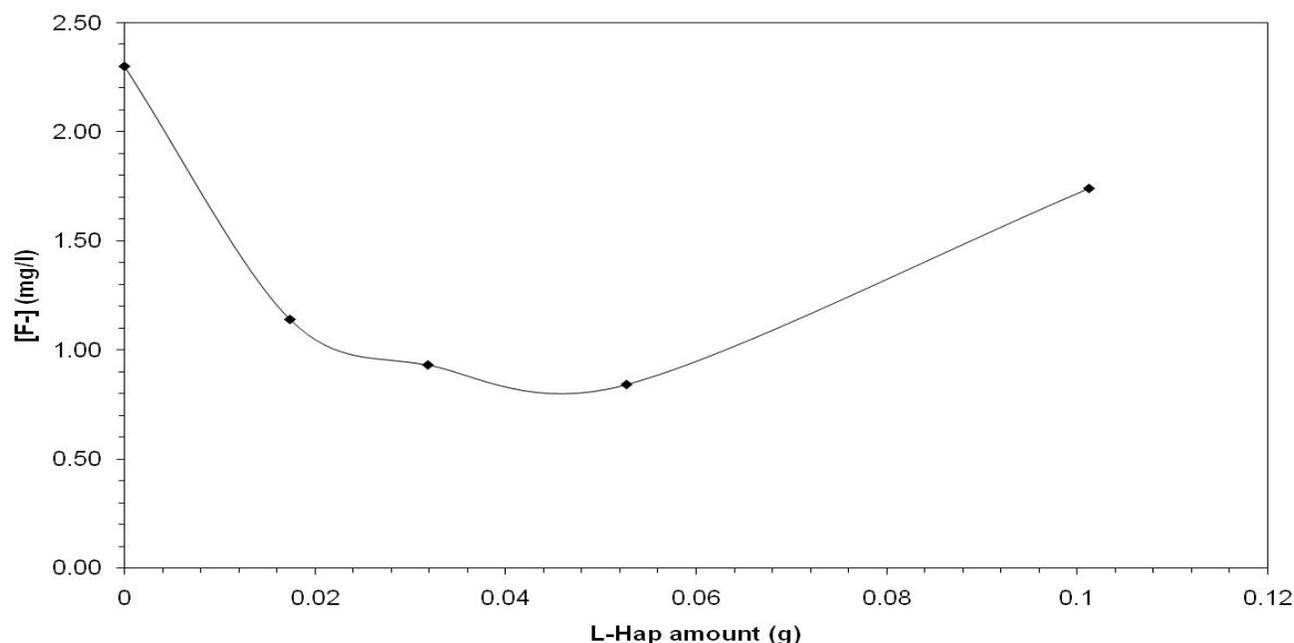
Figure 15. The evaluation of fluoride concentration of Koundoumawa field water during the defluoridation: Effect of sorbent dose of precipitated L-HAp.

continuously with an increasing dose of the L-Hap sorbent, contrary to synthetic solution. With the fluoride poisoning Koundoumawa field water, the defluoridation by L-Hap sorbent is mainly controlled by the dissolution-and-recrystallization mechanism, contrary to synthetic solution, where ion exchange is the dominant pheno-menon. The minimum pH obtained is 6.5 for 0.1012 g of sorbent.

The evaluation of fluoride ion concentration with sorbent dose is shown in Figure 15. We observed that the fluoride ion concentration decreases with an increasing dose of sorbent. This phenomenon is still observed until the addition of 0.0527 g amount of L-Hap sorbent dose. The minimum fluoride ion concentration reached is 0.84 mg/l. This value satisfies the level of fluoride within the tolerance limit (WHO guideline value = 0.8 mg/l). After this dose, there is an increase of fluoride concentration, confirming the recrystallization-and-disso-lution mechanism. For 0.0527 g amount of L-Hap sorbent with contact time of 72 h, the fluoride removal capacity of L-Hap is 11.63 mg/g for synthetic water and 2.80 for Koundoumawa field water. We can conclude that the presence of high concentration of bicarbonate ion in Koundoumawa field water is responsible of this low fluoride removal capacity of L-Hap during defluoridation of this water. Similar results for bicarbonate ion have also been reported (Dilip et al., 2010; Sairam et al., 2008; Sanjay et al., 2009).

Conclusion

From the present results, we can conclude as follows:

1. DCPD and L-Hap sorbents are appropriate for the defluoridation of synthetic solutions and Koundoumawa fluoride poisoning field waters.
2. The DCPD shows higher fluoride uptake capacity for defluoridation of synthetic water as compared to L-HAp. The uptake of fluoride in acidic pH is higher as compared to alkaline pH for synthetic solution.
3. The L-HAp shows higher fluoride uptake capacity for fluoride poisoning Koundoumawa field waters as compared to DCPD.
4. Within the first two hours, the sorption process is essentially controlled by ion exchange mechanism.
5. From 2 to 20 h, the sorption process is controlled by the dissolution-and-recrystallization mechanism.
6. From 20 to 72 h, the sorption process is again controlled by ion exchange mechanism.
7. The fluoride removal capacity of DCPD and L-hap decreases with a raise in sorbent dose contrary to the fluoride ion concentration.
8. With the fluoride poisoning Koundoumawa field water, the defluoridation by L-Hap sorbent is mainly controlled by the dissolution-and-recrystallization mechanism, contrary to the synthetic solution, where ion exchange is the dominant phenomenon.

Conflict of interests

The authors did not declare any conflict of interest.

REFERENCES

Amit B, Eva K, Mika S (2011). Fluoride removal from water by adsorption - A review. Chem. Eng. J. 171(3):811-840.

Anirudhan TS, Maya RU (2007). Arsenic(V) removal from aqueous solutions using an anion exchanger derived from coconut coir pith and its recovery. Chemosphere, 66(1):60-66.

Boualia A, Mellah A, Aissaoui T, Menacer K, Silem A (1993). Adsorption of organic matter contained in industrial H_3PO_4 onto bentonite: batch-contact time and kinetic study, Appl. Clay Sci. 7:431-445.

Brown WE, Lehr JR (1959). Applictation of phase rule to the chemical behaviour of MCPM in soils. Soil Sci. Soc. Amer. Proc. 23:7-12.

Casciani FS, Condrate SrRA (1980). The infrared and Raman Spectra of Several Calcium Hydrogen Phosphates, Proc. 2nd Internatl., Congress on Phosphorus compounds, Boston, pp.175-190.

Chow LC, Markovic MI (1997). Calcium phosphates in biological and industrial systems. Boston: Kluwer Academic Publishers, pp. 67-84.

Diaz-Nava C, Olguin MT, Solache-Rios M (2002). Water defluoridation by Mexican heulandite-clinoptilolite, Sep. Sci. Tech. 37:3109-3128.

Dilip T, Sadhana R, Raju V, Siddharth M, Subrt J, Nitin L (2010). Magnesium incorporated bentonite clay for defluoridation of drinking water. J. Hazard. Mater. 180:122-130.

Fan X, Parker DJ, Smith MD (2003). Adsorption kinetics of fluoride on low cost materials, Water Res. 37:4929-4937.

Featherstone JDB, Glena R, Shariati M, Shields CP (1990). Dependence ofiln vitro demineralization of apatite and remineralization of dental enamel on fluoride concentration. J. Dent. Res. 69:620-625.

Hammari LEL, Laghzizil A, Barboux P, Lahlil K, Saoiabi A (2004). Retention of fluoride ions from aqueous solution using porous hydroxyapatite: structure and conduction properties, J. Hazard. Mater. 114:41-44.

JCPDS (Joint Committee on Powder Diffraction Standards) cards, (DCPD card number 09-0077).

JCPDS (Joint Committee on Powder Diffraction Standards) cards, (L-Hap card number 9-432).

Jiménez-Reyes M, Solache-Ríos M (2010). Sorption behavior of fluoride ions from aqueous solutions by hydroxyapatite, J. Hazard. Mater. 180(1-3):297-302.

Kalimuthu P, Natrayasamy V (2014). Synthesis of alginate bioencapsulated nano-hydroxyapatite composite for selective fluoride sorption. Carbohydrate Polymers, 112:662-667.

Kamble SP, Jagtap S, Labhsetwar NK, Thakare D, Godfrey S Devotta S, Rayalu SS (2007). Defluoridation of drinking water using chitin, chitosan and lanthanum-modified chitosan. Chem. Eng. J. 129:173-180.

Kevin JR, Kenneth TS (2014). Measurement of fluoride substitution in precipitated fluorhydroxyapatite nanoparticles. J. Fluorine Chem. 161:102-109.

Larsen MJ, Pearce EIF, Jensen SJ (1993). Defluoridation of Water at High pH with Use of Brushite, Calcium Hydroxide, and Bone Char. J. Dent. Res. 72:15-19.

LeGeros RZ, Lee D, Quirolgico G, Shirra WP, Reich L (1983). In vitro formation of Dicalcium Phosphate Dihydrate $CaHPO_4.2H_2O$, Scanning Electron Microscopy, pp. 407-418.

Lerch P, Lemp R, Kraheebuhl U, Bosset J (1966). Etude de l'hydrolyse de l'orthophosphate dicalcique dihydrat´e. Chimia, 20:430-432.

Low KS, Lee CK, Leo AC (1995). Removal of metals from electroplating wastes using banana pith, Bioresour. Technol. 51:227-231.

Lusvardi G, Malavasi G, Menabue L, Saladini M (2002). Removal of cadmium ion by means of synthetic hydroxyapatite,Waste Manag. 22:853-857.

Maiti GC, Freund F (1981). Influence of fluorine substitution on the proton conductivity of hydroxyapatite. J. Chem. Soc. Dalton Trans. 4:949-955.

Mameri N, Yeddou AR, Lounici H, Lounici D, Belhocine H, Grib BB (1998). Defluoridation of serprntrional Sahara water of North Africa by electrocoagulation process using bipolar aluminium electrodes, Water Res. p.32.

Manzola AS, Mgaidi A, Laouali MS, El Maaoui M (2014). On precipitated calcium and magnesium phosphates during hard waters softening by monosodium phosphate. Desalination and water treatment: 52(25-27):4734-4744.

Masamoto T, Tetsuji C (2004). Reaction between calcium phosphate and fluoride in phosphogypsum. J. Eur. Ceramic Soc. 26(4-5):767-770.

Masanobu K, Ryohei I, Koji I (2013). Preparation and evaluation of spherical Ca-deficient hydroxyapatite granules with controlled surface microstructure as drug carriers. Mat. Sci. Eng. C. 33(4):2446-2450.

Medellin-Castillo NA, Leyva-Ramos R, Padilla-Ortega E, Ocampo-Perez R, Flores-Cano JV, Berber-Mendoza MS (2014). Adsorption capacity of bone char for removing fluoride from water solution. Role of hydroxyapatite content, adsorption mechanism and competing anions. J. Indus. Eng. Chem. 20(6):4014-4021.

Meenakshi S, Anitha P, Karthikeyan G, Appa Rao BV (1991). The pH dependence of efficiency of activated alumina in defluoridation of water, Indian. J. Environ. Prot. 11:511-513.

Meenakshi S, Viswanathan N (2007). Identification of selective ion exchange resin for fluoride sorption, J. Colloid Interface Sci. 308:438-450.

Mourabet MM, El Rhilassi A, El Boujaady H, Bennani-Ziatni M, El Hamri R, Taitai A (2012). Removal of fluoride from aqueous solution by adsorption on hydroxyapatite (HAp) using response surface methodology, J. Saoudi Chem. Soc. doi:10.1016/j.jscs.2012.03.003.

Nash CL, Liu JC (2010). Removal of phosphate and fluoride from wastewater by a hybrid precipitation–microfiltration process. Separation and Purification Technology, 74(3):329-335.

Okazaki M, Aoba T, Doi Y, Takahashi J, Moriwaki J (1981). Solubility and crystallinity in relation to fluoride content of fluoridated hydroxyapatites. J. Dent. Res. 60:845-849.

Okazaki M (1992). Heterogeneous synthesis of fluoridated hydroxyapatites. Biomat.13:749-754.

Rapport Mission Internationale d'Enquête de la Fédération Internationale des Ligues des Droits de l'Homme (2002), N° 341 octobre.

Rao NV, Mohan R, Bhaskaran CS (1998). Studies on defluoridation of water, J. Fluorine Chem. 41:17-24.

Sairam CS, Natrayasamy V, Meenakshi S (2008). Defluoridation chemistry of synthetic hydroxyapatite at nano scale: Equilibrium and kinetic studies, J. Hazard. Mater. 155(1-2):206-215.

Sandrine B, Ange N, Didier B, Eric C, Patrick S (2007). Removal of aqueous lead ions by hydroxyapatite: equilibria and kinetic process, J. Hazard. Mater. 139:443-446.

Sanjay PK, Priyadarshini D, Sadhana SR, Nitin KL (2009). Defluoridation of drinking water using chemically modified bentonite clay. Desalination 249(9):687-693.

Sekar C, Kanchana P, Nithyaselvi R, Girija EK (2009). Effect of fluorides (KF and NaF) on the growth of dicalcium phosphate dihydrate (DCPD) crystal. Mater. Chem. Phys. 115(1):21-27.

Smiciklas I, Dimovic S, Plecas I, Mitric M (2006). Removal of Co^{2+} from aqueous solutions by hydroxyapatite, Water Res. 40:2267-2274.

Sumit G, Rajkamal B, Sampath KTS (2012). Effects of nanocrystalline calcium deficient hydroxyapatite incorporation in glass ionomer cements. J. Mechan. Behav. Biomed. Mater. 7:69-76.

Sundaram CS, Natrayasamy V, Meenakshi S (2008). Uptake of fluoride by nano-hydroxyapatite/chitosan, a bioinorganic composite. Bioresource Technology, 99(17): 8226-8230.

Taewook Y, Chulki K, Jaeyoung J, Il Won K (2012). Regulating fluoride uptake by calcium phosphate minerals with polymeric additives. Colloids and Surfaces A: Physicochem. Eng. Aspects 401:126-136.

Takahashi T, Tanase S, Yamamoto O (1978). Electrical conductivity of some hydroxyapatites. Electrochim Acta. 23:369-373.

Tse-Ying Liu, San-Yuan Chen, Dean-Mo Liu, Sz-Chian Liou (2005). On the study of BSA-loaded calcium-deficient hydroxyapatite nano-carriers for controlled drug delivery. J. Contr. Release 107(1):112-121.

UNICEF (1998). Fluoride in water: An overview." WES (Warter Environment & Sanitation) Section, Programme Division, UNICEF 3 UN Plaza, New York, NY, USA 10017 Phone: (212) 824-6000 Fax: (212) 824-6480

Vega ED, Pedregosa JC, Narda GE, Morando PJ (2003). Removal of oxovanadium (IV) from aqueous solutions by using commercial crystalline calcium hydroxyapatite, Water Res. 37:1776-1782.

World Health Organisation (WHO) (1996). Fluoride, Guidelines for Drinking Water Quality, vol. II, 2nd ed., Geneva, pp. 231-237.

Wen L, Lei Z, Longhua P, Christian R (2011). Fluoride removal performance of glass derived hydroxyapatite. Mater. Res. Bull. 46(2):205-209.

Xiaolin Y, Shengrui T, Maofa G, Junchao Z (2013). Removal of fluoride from drinking water by cellulose@hydroxyapatite nanocomposites. Carbohydr. Polymers 92(1):269-275.

Yulun N, Chun H, Chuipeng K (2012). Enhanced fluoride adsorption using Al (III) modified calcium hydroxyapatite. J. Hazard. Mater. pp. 233-234:194-199.

Yu W, Ningping C, Wei W, Jing C, Zhenggui W (2011). Enhanced adsorption of fluoride from aqueous solution onto nanosized hydroxyapatite by low-molecular-weight organic acids, Desalination, 276(1-3):161-168.